



Research Article

Synthesis and Applications of Green Synthesized TiO₂ Nanoparticles for Photocatalytic Dye Degradation and Antibacterial Activity

Annin K. Shimi ¹, **Hiwa M. Ahmed** ^{2,3}, **Muhammad Wahab**⁴, **Snehlata Katheria**⁵, **Saikh Mohammad Wabaidur**⁶, **Gaber E. Eldesoky**^{6,7}, **Md Ataul Islam**⁷, and **Kantilal Pitamber Rane**⁸

¹Department of Physics, Manonmaniam Sundaranar University, Tirunelveli, Tamilnadu-627012, India

²Sulaimani Polytechnic University, Slemani, 46001 Kurdistan Region, Iraq

³Department of Horticulture, University of Raparin, Ranya, Kurdistan Region, Iraq

⁴Food Science and Quality Control Department, College of Agricultural Engineering Science, University of Sulaimani, Slemani, Kurdistan Region, Iraq

⁵Department of Chemistry, University of Lucknow, Lucknow-226007, Uttar Pradesh, India

⁶Department of Chemistry, College of Science, King Saud University, Riyadh-11451, Saudi Arabia

⁷Division of Pharmacy and Optometry, School of Health Sciences, Faculty of Biology, Medicine and Health, University of Manchester, Manchester, UK

⁸Electronics and Communication Engineering Department, KL University, Hyderabad, India

Correspondence should be addressed to Hiwa M. Ahmed; hiwa2009@yahoo.com

Received 2 January 2022; Revised 27 January 2022; Accepted 14 February 2022; Published 2 March 2022

Academic Editor: Wenhui Zeng

Copyright © 2022 Annin K. Shimi et al. This is an open access article distributed under the Creative Commons Attribution License, which permits unrestricted use, distribution, and reproduction in any medium, provided the original work is properly cited.

Metal oxide photocatalyst is one of the promising photocatalysts in the water remediation process. The present work is aimed at synthesizing the green production of TiO₂ (G-TiO₂) nanoparticles from mulberry plant extract. Plant phytochemicals serve a different role to produce the nanophase particles. The bioreductant is safer and noxious free compound for synthesizing the G-TiO₂ nanoparticles. The synthesized G-TiO₂ nanoparticles in anatase phase and their crystallite size of 24 nm were characterized from X-ray diffraction analysis. The Ti-O bonding and plant derivatives and their reduction were confined from FTIR analysis. The wide bandgap of G-TiO₂ nanoparticles (3.16 eV) and their optical characterization were captured from UV-DRS analysis. The spherical surface morphology and their Ti and O elemental configurations were characterized from FESEM with EDX technique. The photocatalytic dye degradation was examined against methylene blue dye, and their pseudo-first-order kinetics were evaluated. The cyclic experiments declared their catalytic potential. The bacterial resistance of G-TiO₂ nanoparticles was examined against gram-positive and gram-negative bacteria. Hence, the catalytic potential and bacterial stability of G-TiO₂ nanoparticles are the powerful candidate for water remediation and biomedical applications.

1. Introduction

The phrase “nanotechnology” refers to the design, manufacture, and application of functional structures with at least one characteristic dimension measured in nanometers [1]. Catalysis, optical, electric, and magnetic characteristics, diagnostics, biological probes, and display devices are all

areas where metal oxide nanoparticles have a lot of potentials [2]. Due to their simple production and eco-loving nature, there is no need of high-cost equipment setup. Recently, green production of nanomaterials was the focus of the researchers [3, 4]. Metallic nanoparticles are synthesized in two ways: top-down and bottom-up, via chemical, physical, and biological methods. The bottom-up technique

follows the combining of atoms to generate bulk nanoparticles, while the top-down method follows the method of transforming bulk materials to nanoparticles [5]. They have also been used as chemical reaction catalysts, biosensors, antioxidants, and DNA delivery. The peculiar properties of nanoparticles, such as their stability, catalytic activity, biocompatibility, high conductivity, and strong surface area-to-volume ratio, could be due to these diverse activities. Instead of the toxic materials used in chemical and physical synthesis, the green synthesis of nanomaterials utilizing plants/plant component extracts had played a vital role in the field of nanotechnology out of all the approaches enumerated. The green synthesis of NPs can be accomplished by using the metabolites of bacteria, fungi, yeast, algae, actinomycetes, and plants as reducing and capping agents. Green synthesis of nanoparticles has gotten more publicity, because of its low cost, simplicity, scalability, eco-friendliness, and the wide range of metabolites secreted by plants. Plant products such as leaves, bark, roots, stems, peels, and other biological resources are accessible in nature and could be used for the green production of nontoxic nanoparticles. Traditional Indian medical systems rely heavily on medicinal herbs. The importance of medicinal plants as a possible source of bioactive chemicals has been recognized in pharmacological investigations [6]. Medicinal plants have been discovered to be effective in the treatment of a variety of health issues over time. *Morus alba* Linnaeus is one of those species in the Moraceae family. The majority of the species are endemic to Asia, for which the environment is warm. It is used as traditional medicine and modern drug preparation, mainly constitutes diet for the silkworm [7, 8]. Phytochemicals are compounds found in medicinal plants, leaves, vegetables, and roots that act as a defense mechanism and provide protection against a variety of ailments. Primary and secondary compounds are referred to as phytochemicals. Primary ingredients include chlorophyll, proteins, and simple carbohydrates, whereas secondary chemicals include terpenoids, alkaloids, and phenolic chemicals. Many health concerns, such as cancer, heart disease, diabetes, and high blood pressure, are being pushed for the prevention and treatment of phytochemicals [9–12]. *Morus* plant has shown strong antifungal activities. *M. alba* has garnered great attention for its antioxidative and antidiabetic effects [13]. *M. alba* has antioxidant, antibacterial, antiviral, and anti-inflammatory properties [14, 15]. The mulberry extract using nanoparticles exhibited the enhanced bacterial activity [16–21]. The present work reports the green production of TiO_2 (G- TiO_2) nanoparticles and their bacterial activity and catalytic dye degradation activity.

2. Materials and Methods

2.1. Materials. Titanium tetra isopropoxide-Analytical Reagent (TTIP-AR) solution was purchased from Sigma Aldrich, India. The methylene blue dye was purchased from HiMedia, India. The fresh mulberry leaves were collected from Kanyakumari market, Tamilnadu, India. The procured materials were used without further modifications

to synthesize the nanoparticles, and the solvent is double distilled water.

2.2. Preparation of Mulberry Plant Extract. The collected fresh mulberry leaves (10 g) were washed with running water. The purified leaves were combined with 100 mL double distilled water. The combined compounds were heated by using magnetic stirrer at 100°C for 10 minutes, and the remaining impurities were removed by using Whatman No. 1 filter paper (HiMedia, Mumbai). The collected solutions were stored for refrigerator at 4°C for further analysis.

2.3. Nano Production of G- TiO_2 Nanoparticles. One molar concentration of TTIP solution was mixed with 10 mL mulberry plant extract to synthesize the G- TiO_2 nanoparticles. The combined solution was stirred by using magnetic stirrer at 80°C temperature and 800 rpm. The milk white precipitate was formed in 30 minutes, and the colour formations were evident of the nanophase materials. The white participate solutions were centrifuged at 15000 rpm for 10 minutes, and the same process was repeated for three times. The centrifuged samples were filtered by Whatman No. 1 filter paper. The collected samples were heated at 100°C for 1 hour. The dried samples were stored in desiccator for further characterizations.

2.4. Characterization of G- TiO_2 Nanoparticles. The crystalline structure and sizes were captured from X-ray diffractometer (PANalytical XPert-Cu $K\alpha$ radiation) worked in 30 KV and 40 mA. The plant compounds and their functional groups and metal bonding were derived from FTIR (Perkin Elmer) spectroscopy. The optical information was determined from UV-DRS (Shimadzu-2700) analysis. The surface shape and their exiting elements were characterized from FESEM with EDX (Carl Zeiss) analysis.

2.5. Antibacterial Activity. The synthesized G- TiO_2 nanoparticle bacterial activities were evaluated by using gram-positive *Staphylococcus aureus* (ATCC 6538) and gram-negative *Escherichia coli* (ATCC 8739) over the well diffusion method. The nutrient broth was inoculated by bacterial culture (10^6 CFU/mL), and inoculated suspensions were incubated for 24 hours. The incubated suspensions were swabbed over the Mueller-Hinton-mediated petri plates. The gel puncture was used to make the well about 5 mm on agar-mediated petri plates, and the same concentrations (20 $\mu\text{g}/\text{ml}$) were put it over the well. The loaded petri plates were incubated for overnight at 37°C. Finally, the incubated samples exhibited the zones around the well. The bacterial inactivity was measured by zone of inhibitions in the range of millimeter scale. The bacterial inactivity of G- TiO_2 nanoparticles was compared with the same concentration of mulberry plant extract and antibiotic drug (gentamycin-SD195 Gentamicin, 120 micrograms).

2.6. Photocatalytic Activity. The photocatalytic activity of synthesized G- TiO_2 nanoparticles was evaluated by methylene blue dye under UV light irradiation (wavelength = 300 nm). 10 ppm dye solution was used in the catalytic activity. The 100 mL MB dye solution was mixed with 10 mg

nanocatalyst of G-TiO₂ nanoparticles. The combined catalyst solution was stirred under dark condition by using magnetic stirrer. The dark conditions help to achieve the adsorption-desorption equilibrium position. The combined solutions were kept in a UV chamber and light irradiated for 120 minutes. For the periodic intervals (30 minutes), the irradiated solution was taken out for 5 mL to measure the degradation efficiency. The collected dye solutions were centrifuged at 10000 rpm for 5 minutes to eliminate the unwanted elements and nanocatalyst. The centrifuged samples were measured for UV-Visible spectroscopy. The same working procedure was followed by reusability analysis. The dye degradation efficacy was characterized from below mentioned equation as follows:

$$\text{Photocatalytic dye degradation (\%)} = \frac{(C_0 - C_t)}{C_0} \times 100, \quad (1)$$

where the initial dye concentration is C₀ (without UV light irradiation) and the concentration of the dye at different UV light irradiation time is C_t. The free radicals and holes are measured from the quenching experiment. The p-benzoquinone (BQ) was used to determine the superoxide ion activity, isopropyl alcohol (IPA) was used to find the hydroxyl activity, and triethanolamine (TEOA) was used to analyze the hole activity in the catalytic activity. These compounds restrict the free radicals, holes, and superoxides, and their concentration is 1 mmol/L.

3. Results and Discussion

3.1. XRD Analysis. The phase, purity, and structural average crystallite size values of amalgamated G-TiO₂ nanoparticles were observed by the XRD pattern exhibited in Figure 1. The X-ray diffraction peaks examined at 25.38°, 37.97°, 48.14°, 54.40°, 55.20°, 62.71°, 68.51°, 71.71°, and 75.30° correspond to Miller index (hkl) value of (101), (004), (200), (105), (211), (118), (116), (220), and (315), respectively. The collected outcomes were verified utilizing JCPDS Card No. 78-2486 (Joint Committee on Powder Diffraction Standards) [22]. The photocatalytic activity is improved by the crystallinity of the nanoparticles, as evidenced by a strong peak. The regular crystalline size of the particle was evaluated utilizing Debye Scherrer's equation is given by $D = 0.89\lambda/\beta \cos \theta$ [23]. To evaluate the crystalline size, the (101) plane was selected. The as-prepared TiO₂ nanoparticles elicited utilizing mulberry solution had an average crystalline size of approximately 22 nm, which was measured by repeating the experiment 3 times with standard deviation (SD) value ± 0.024 . The surface area [23] of the catalyst is $7.33 (\times 10^5 \text{ g/cm}^2)$. As an outcome, it is determined that TiO₂ nanoparticles possess a tremendous surface area and dye molecules on their surface, which might be responsible for occurring in better photocatalytic performance.

3.2. FTIR Analysis. Figure 2 shows the FTIR spectra of G-TiO₂ nanoparticles synthesized from mulberry plant extract green chemical-reduction method. The strong absorption peak at 1633 cm^{-1} and 3428 cm^{-1} is responsible for the OH

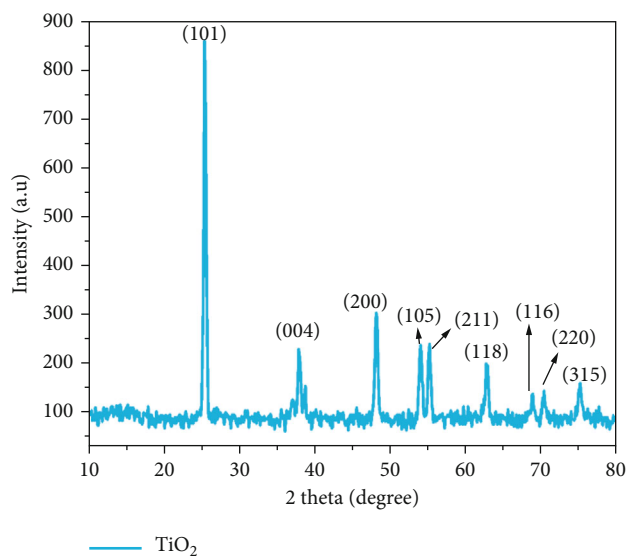


FIGURE 1: XRD diffraction pattern of synthesized G-TiO₂ nanoparticles.

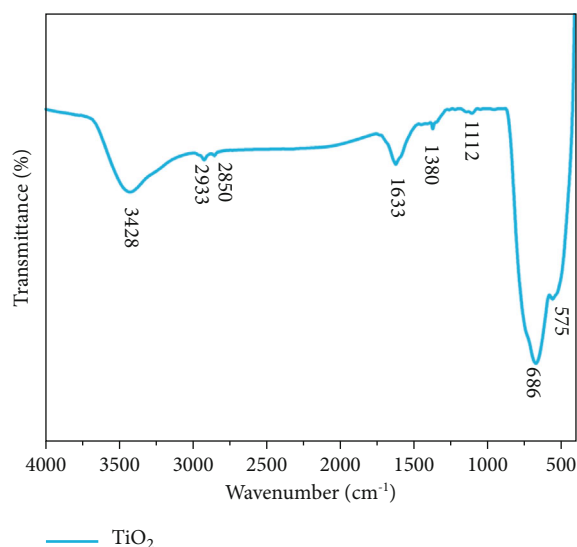


FIGURE 2: FTIR spectrum of synthesized G-TiO₂ nanoparticles.

groups [24]. The peaks which are 2933 cm^{-1} and 2850 cm^{-1} attribute the C-H stretching which confirmed the organic compound reduction from the surface [25]. The peak at 1380 cm^{-1} represents the plant biocompounds and their C-C bond stretching and C-O bond stretching from the plant extract [26]. The metal-oxygen peak at 686 cm^{-1} represents O-Ti-O bonding in cationic anatase phase [27]. The plant extract and metallic peaks responsible for band assignment were derived from FTIR analysis. The phenolic compounds from the plant extract serve a bioreductant to synthesis G-TiO₂ nanoparticles.

3.3. UV-DRS Analysis. The green production of G-TiO₂ nanoparticle optical endurance was measured from UV-DRS analysis. The optical absorption edge is located at

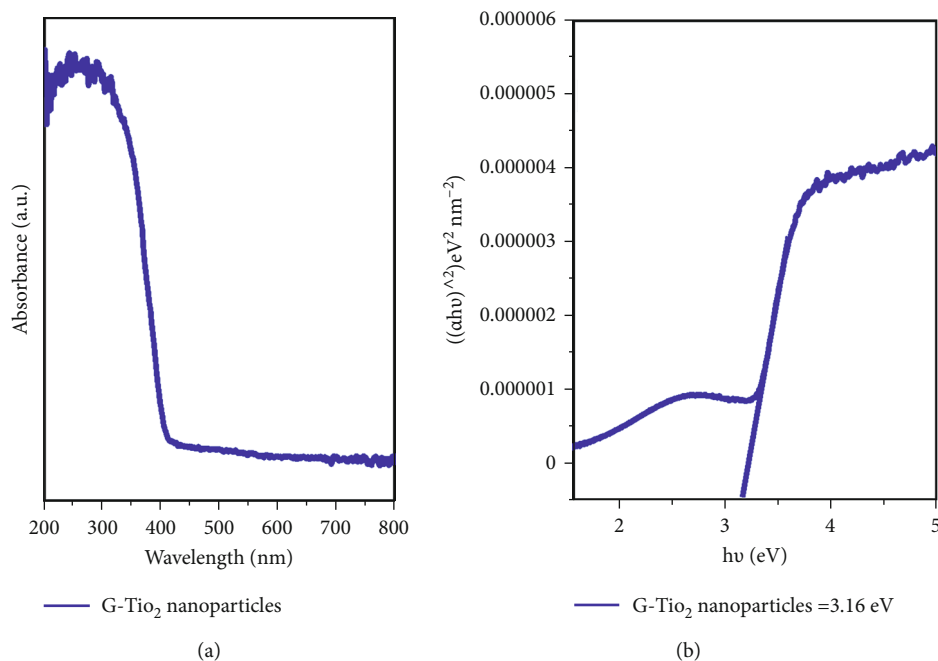


FIGURE 3: (a) UV-DRS absorption and (b) bandgap energy spectrum of synthesized G-TiO₂ nanoparticles.

around 398 nm (Figure 3(a)) which acknowledges the transition of electrons from valence band to conduction band (O-2p to Ti-3d) [28]. The high valency Ti-3d orbitals were suppressed by 2-p orbitals from oxide compounds. The photoexcited electrons and electrons are recombined each other. The excited electrons were restricted by oxide compounds, and their recombination was suppressed. The charge transformation decreased the recombination activity and extended their life time [29]. These activities increase the light absorption activity. The optical bandgap energy was detected from the Kubelka-Munk equation. The obtained bandgap values are displayed in Figure 3(b). The wide bandgap of G-TiO₂ nanoparticles restricts the charge carriers and promotes the carrier production. The separated charge carriers promote the extension of e-h pair activity. The wide bandgap is one of the key factors for better photocatalytic activity. The suppressed charge carriers increased the reactive oxygen species and hydroxyl radical formations [30]. These productions promote the reduction of pollution from environment through the photocatalysis and bacterial degradation activity.

3.4. FESEM with EDX Analysis. Figure 4 displays the FESEM images and EDX values of G-TiO₂ nanoparticles. The size, shape, and elemental compositions were captured from FESEM analysis. The FESEM images of G-TiO₂ nanoparticles showed a spherical shape and conjoint spherical shapes with the size of 24 nm. The spherical shape is one of the largest surface area shapes than another nanostructure [31]. The conjoint spherical shapes are attained from the plant extract on the surface G-TiO₂ nanoparticles. The excessive amount of plant extracts was reassured from FTIR spectroscopy. The title materials were identified from EDX analysis shown in Figures 4(c) and 4(d). The EDX spectrum derived the Ti

and O peaks with respect to the energy levels. The Ti has major peaks than O. The atomic and weight percentage of G-TiO₂ nanoparticles represent the Ti and O. The O presence is very important for radical formation. The formed radicals are broadly applicable in biological and water remediation process.

3.5. Antibacterial Activity. Figure 5 represents the antibacterial activity of G-TiO₂ nanoparticles. The bacterial inactivity was measured by zone of inhibitions which is displayed in Figure 5. The antibacterial activity of G-TiO₂ nanoparticles against gram-positive (*S. aureus*) and gram-negative (*E. coli*) bacterial strains was compared with antibiotic drug gentamycin and mulberry plant extract. The G-TiO₂ nanoparticles own the high valency Ti³⁺ and dissolved oxygen compounds which can restrict the cell production. The dissolved oxygen provokes the free radical generation and superoxide formation [32–34]. These actions can disconnect the electron transfer to the cell system. The disconnected electron supply miscommunicates the cell production which can lead a cell demise. The gram-positive bacterial strain is more sensitive than gram-negative bacteria due to their weak cell wall membrane.

3.6. Photocatalytic Activity. A significant quantity of trash is created throughout numerous dyeing and finishing operations. Humans, microbes, and aquatic species are all poisoned by dye-containing discharge pollutants. When these colours are released into rivers or lakes, they create unsightly pollution, physiologically increasing eutrophication, toxicity, and disruption in aquatic life. Traditional water treatments are not completely degrading the dyes because such colours are chemically stable [35–37].

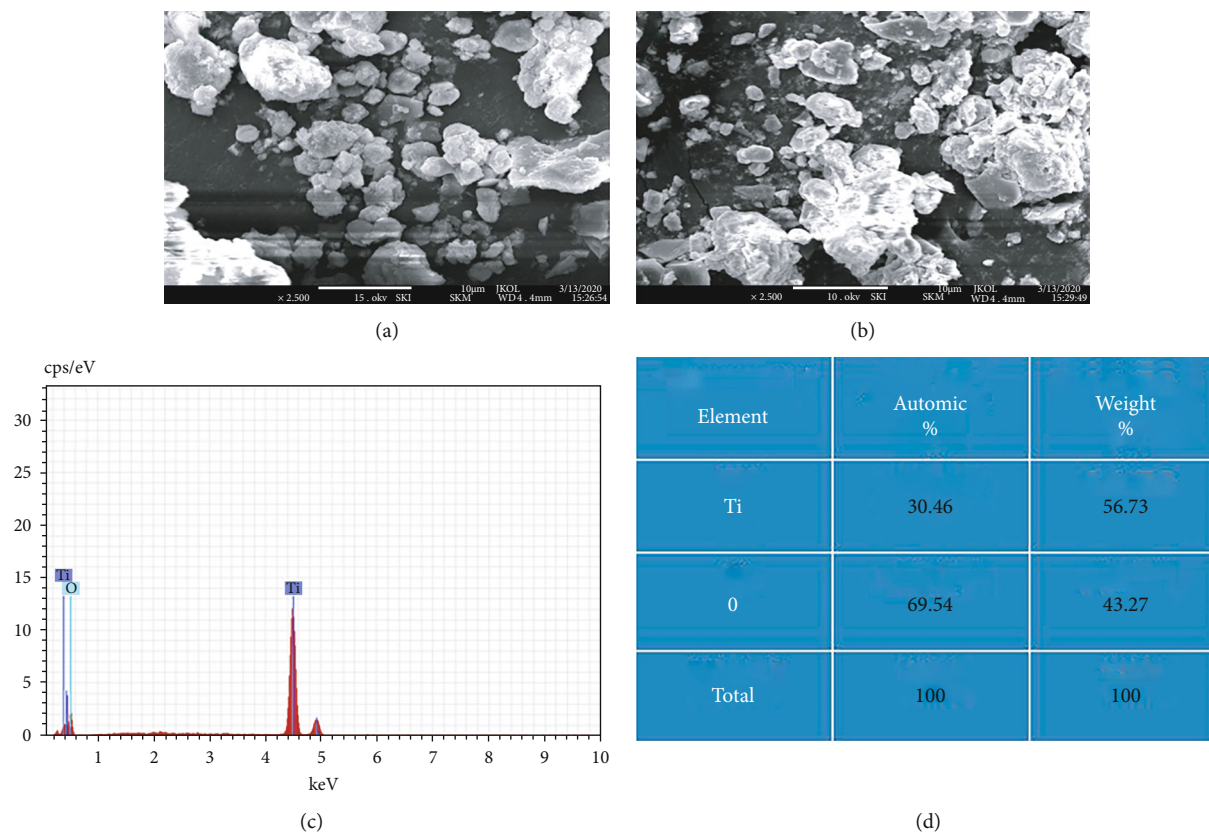


FIGURE 4: (a, b) FESEM images, (c) EDX spectra, and (d) EDX table of the G-TiO₂ nanoparticles.

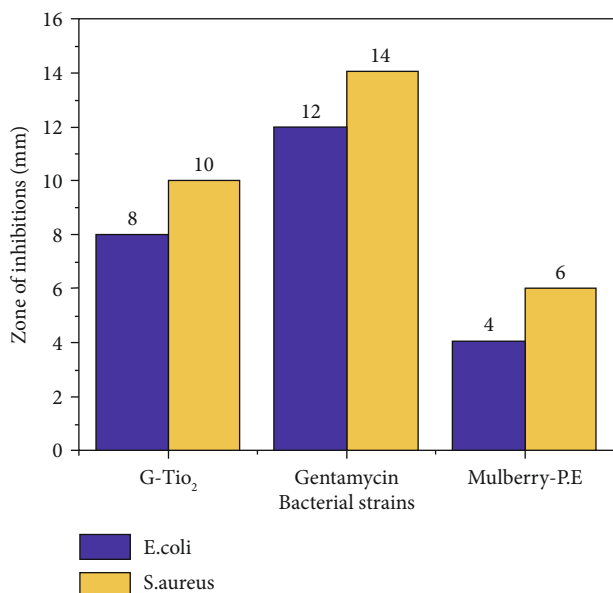


FIGURE 5: Antibacterial activity of synthesized G-TiO₂ nanoparticles.

The UV light-irradiated MB dye degradation spectrum is shown in Figure 6. The dye degradation without catalyst is shown in Figure 6(a). The degradation is 6% which is very lower degradation efficiency. The catalytic degradation efficiency was found to be very high from 0 min to 30 min and reached to a maximum of 96% at 120 min due to the

presence of G-TiO₂ nanoparticles (Figure 6(b)). It might be due to the huge surface area of the materials [25–29]. The C/C₀ spectrum and pseudo-first-order kinetics spectrum show the catalytic activity of G-TiO₂ nanoparticles in Figures 6(b)–6(d). For improved oxidative breakdown of colours in wastewater, a UV radiation combination has been applied. UV reactions degrade the chromophoric structure of such dyes, resulting in complete decolourization. The superoxides have more power than the holes and hydroxyl ions which is displayed in Figure 6(e). The O₂^{•-} molecules strongly degrade the MB dye molecules and holes and hydroxyl radical are associated part in the catalytic reaction of G-TiO₂ nanoparticles. The G-TiO₂ nanoparticles exhibit excellent catalytic activity due to their adsorbed O₂^{•-} which induced the catalytic stability. The recycle study inferred the catalytic stability and endurance of the G-TiO₂ nanoparticles (Figure 6(f)). When exposed to ultraviolet light, a photon of energy $h\nu$ is emitted; the photon of energy $h\nu$ greater than the band gap stimulates the electron (e⁻) from the valence band to the conduction band and leaves a hole (h⁺) on the valence band, resulting in the production of an electron-hole pair [35–39]. The OH* radical is formed when photogenerated holes on the valence band react with dyes or water attached to the surface. On the photocatalytic dye degradation process, such OH* free radicals are referred to as active species. At the adsorbed molecule, the electron on the conduction band interacts with oxygen to form the anionic superoxide radical O₂^{•-}. The anion O₂^{•-} does not contribute to the oxidation process any longer, but instead react

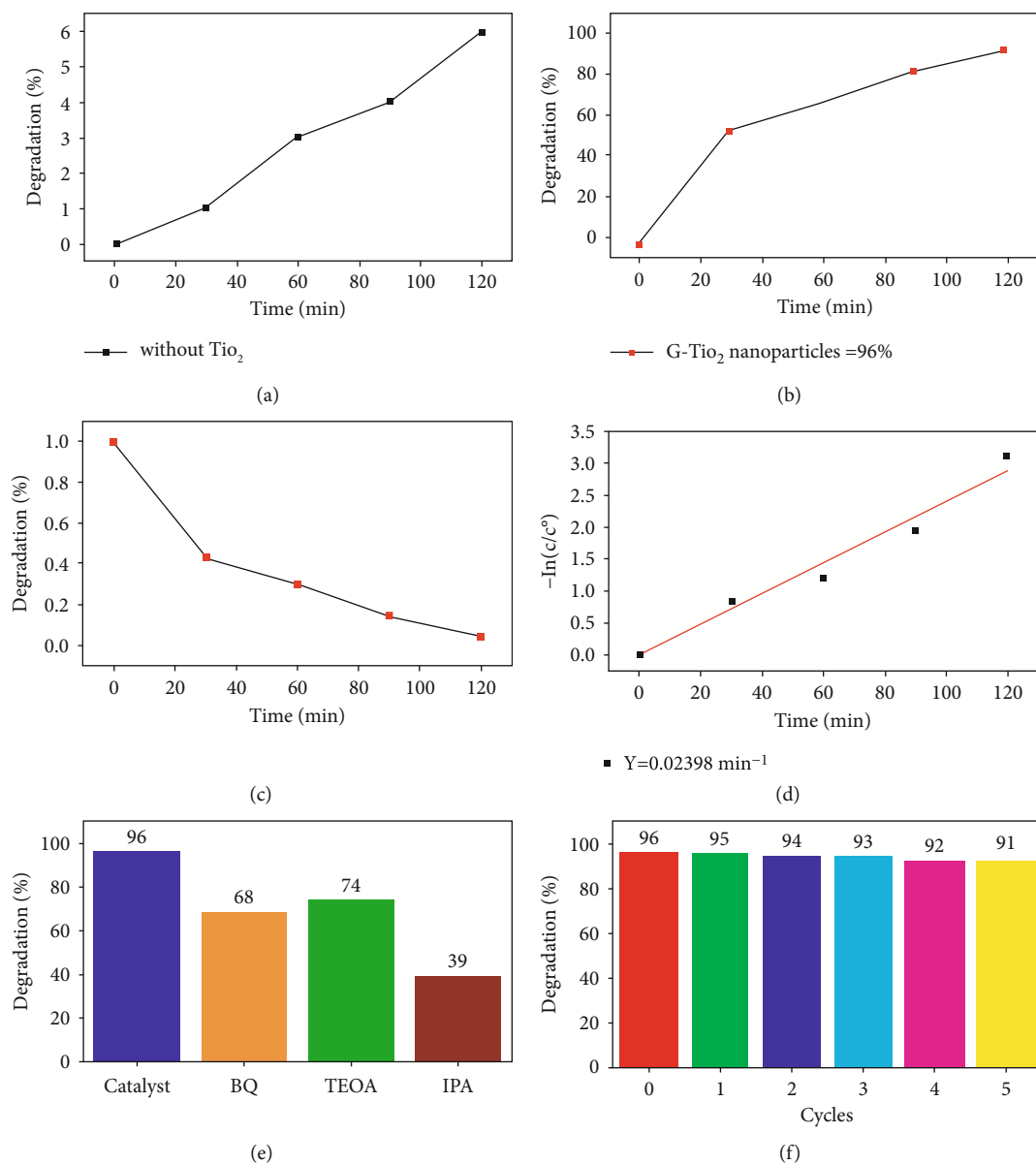


FIGURE 6: (a) Without catalyst dye degradation study, (b) degradation efficiency, (c) C/C_0 absorption rate, (d) photocatalytic degradation kinetics, (e) quenching experiment, and (f) recycle study of the synthesized G-TiO₂ nanoparticles.

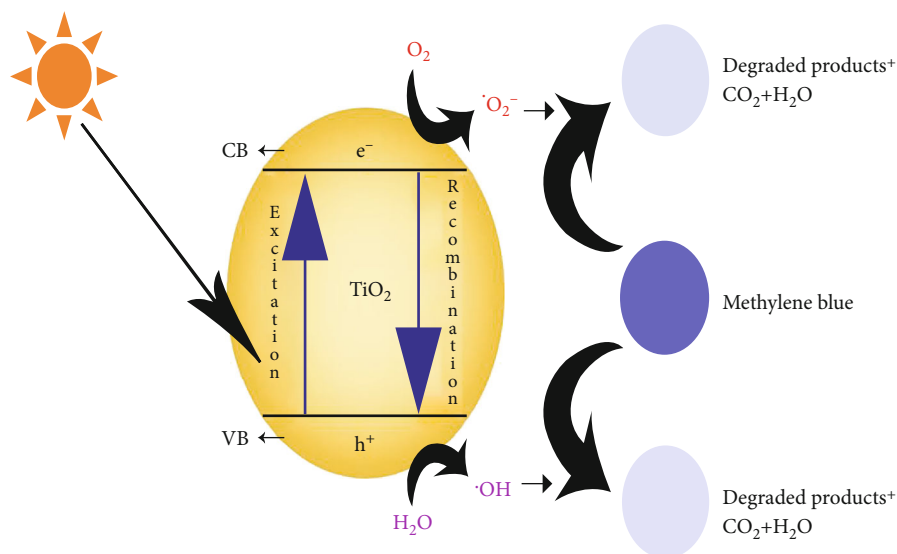


FIGURE 7: Photocatalysis mechanism for G-TiO₂ nanoparticles.

with H⁺ to produce H₂O₂. More trapped electrons are released, resulting in the formation of OH* free radicals. As a result, increasing the creation of electron-hole pairs maximizes the active organism's size and degradation performance [40–44]. The detailed mechanism is shown in Figure 7. The detailed mechanism was derived from the quenching analysis. The photocatalyst stability is displayed in Figure 6(f). According to the results of the current experiment, the performance of samples developed for degrading MB indicates that they can be effective photocatalyst and have an efficient reaction on the degradation of environmental contaminants.

4. Conclusion

The present work effectively synthesized the G-TiO₂ nanoparticles by using mulberry plant extract. The wide bandgap and anatase phase of nanoparticles confirmed the G-TiO₂ nanoparticles. The methylene blue degradation under ultraviolet illumination in 120 minutes exhibited the 96% degradation. The pseudo-first-order kinetics (0.02398 min⁻¹) revealed the catalytic performance of the G-TiO₂ nanoparticles. The reusability of the G-TiO₂ nanoparticles showed the catalytic stability in 5 cycles. The bacterial activity of G-TiO₂ nanoparticles revealed the enriched bacterial sensitiveness against the *S. aureus* bacterial strain. The green nanoproduction is ecological friendly production method, and chemical-free secondary products are released in the outlet. Based on the attained findings, the synthesized G-TiO₂ nanoparticles are suitable for photocatalytic application and microbial resistance-oriented devices.

Data Availability

All research data used to assist the findings of this work are included within the manuscript.

Conflicts of Interest

The authors have no conflict of interests.

Acknowledgments

Authors are grateful to the Researchers Supporting Project No. (RSP-2021/161), King Saud University, Riyadh, Saudi Arabia.

References

- [1] A. Jalill, D. H. Raghad, R. S. Nuaman, and A. N. Abd, "Biological synthesis of titanium dioxide nanoparticles by Curcuma longa plant extract and study its biological properties," *World Scientific News*, vol. 49, no. 2, pp. 204–222, 2016.
- [2] R. Subbaiya, R. S. Lavanya, K. Selvapriya, and M. M. Selvam, "Green synthesis of silver nanoparticles from Phyllanthus amarus and their antibacterial and antioxidant properties," *International Journal of Current Microbiology and Applied Sciences*, vol. 3, no. 1, pp. 600–606, 2014.
- [3] N. I. Rasli, H. Basri, and Z. Harun, "Zinc oxide from aloe vera extract: two-level factorial screening of biosynthesis parameters," *Heliyon*, vol. 6, no. 1, 2020.
- [4] G. Tailor, B. L. Yadav, J. Chaudhary, M. Joshi, and C. Suvalka, "Green synthesis of silver nanoparticles using Ocimum canum and their anti-bacterial activity," *Biochemistry and Biophysics Reports*, vol. 24, 2020.
- [5] M. S. Chavali and M. P. Nikolova, "Metal oxide nanoparticles and their applications in nanotechnology," *SN applied sciences*, vol. 1, no. 6, pp. 1–30, 2019.
- [6] K. Mallikarjuna, S. V. P. Vattikuti, R. Manne et al., "Sonochemical synthesis of silver quantum dots immobilized on exfoliated graphitic carbon nitride nanostructures using ginseng extract for photocatalytic hydrogen evolution, dye degradation, and antimicrobial studies," *Nanomaterials*, vol. 11, no. 11, 2021.
- [7] M. S. Butt, A. Nazir, M. T. Sultan, and K. Schroën, "Morus alba L. nature's functional tonic," *Trends in Food Science & Technology*, vol. 19, no. 10, pp. 505–512, 2008.

- [8] C. C. Chen, L. K. Liu, J. D. Hsu, H. P. Huang, M. Y. Yang, and C. J. Wang, "Mulberry extract inhibits the development of atherosclerosis in cholesterol-fed rabbits," *Food Chemistry*, vol. 91, no. 4, pp. 601–607, 2005.
- [9] H. M. Ahmed, A. Roy, M. Wahab et al., "Applications of nanomaterials in agri food and pharmaceutical industry," *Journal of Nanomaterials*, vol. 2021, Article ID 1472096, 10 pages, 2021.
- [10] H. M. Ahmed, S. Nabavi, and S. Behzad, "Herbal drugs and natural products in the light of nanotechnology and nanomedicine for developing drug formulations," *Mini Reviews in Medicinal Chemistry*, vol. 21, no. 3, pp. 302–313, 2021.
- [11] A. Roy, H. C. Ananda Murthy, H. M. Ahmed, M. N. Islam, and R. Prasad, "Phytogenic synthesis of metal/metal oxide nanoparticles for degradation of dyes," *Journal of Renewable Materials*, vol. 2021, 2021.
- [12] R. Verma, A. Rawat, S. A. Ganie et al., "In vitro antibacterial activity of Cichorium intybus against some pathogenic bacteria," *British Journal of Pharmaceutical Research*, vol. 3, no. 4, p. 767, 2013.
- [13] S. Ahmad, R. Sharma, S. Mahajan, and A. Gupta, "Antibacterial activity of Celtis australis by invitro study," *International Journal of Pharmacy and Pharmaceutical Sciences*, vol. 4, 2012.
- [14] K. O. Chung, B. Y. Kim, M. H. Lee et al., "In-vitro and in-vivo anti-inflammatory effect of oxyresveratrol from Morus alba L.," *Journal of Pharmacy and Pharmacology*, vol. 55, no. 12, pp. 1695–1700, 2003.
- [15] H. A. El-Beshbishy, A. N. B. Singab, J. Sinkkonen, and K. Pihlaja, "Hypolipidemic and antioxidant effects of Morus alba L. (Egyptian mulberry) root bark fractions supplementation in cholesterol-fed rats," *Life Sciences*, vol. 78, no. 23, pp. 2724–2733, 2006.
- [16] S. P. R. Mallem, M. Koduru, K. Chandrasekhar et al., "Potato chip-like 0D interconnected ZnCo2O4 nanoparticles for high-performance supercapacitors," *Crystals*, vol. 11, no. 5, p. 469, 2021.
- [17] S. Some, B. Sarkar, K. Biswas et al., "Bio-molecule functionalized rapid one-pot green synthesis of silver nanoparticles and their efficacy toward the multidrug resistant (MDR) gut bacteria of silkworms (Bombyx mori)," *RSC Advances*, vol. 10, no. 38, pp. 22742–22757, 2020.
- [18] L. N. Liem and D. Nguyen, "Microwave assisted green synthesis of silver nanoparticles using mulberry leaves extract and silver nitrate solution," *Technologies*, vol. 7, no. 1, p. 7, 2019.
- [19] J. Singh, N. Singh, A. Rathi, D. Kukkar, and M. Rawat, "Facile approach to synthesize and characterization of silver nanoparticles by using mulberry leaves extract in aqueous medium and its application in antimicrobial activity," *Journal of Nanostructures Spring*, vol. 7, no. 2, pp. 134–140, 2017.
- [20] A. M. Awwad and N. M. Salem, "Green synthesis of silver nanoparticles by Mulberry leaves extract," *Nanoscience and Nanotechnology*, vol. 2, no. 4, pp. 125–128, 2012.
- [21] L. Xu, W. Li, Q. Shi et al., "Synthesis of mulberry leaf extract mediated gold nanoparticles and their ameliorative effect on Aluminium intoxicated and diabetic retinopathy in rats during perinatal life," *Journal of Photochemistry and Photobiology B: Biology*, vol. 196, 2019.
- [22] G. Ma, X. Chai, G. Hou, F. Zhao, and Q. Meng, "Phytochemistry, bioactivities and future prospects of mulberry leaves: a review," *Food Chemistry*, vol. 372, 2022.
- [23] B. Liu, H. Zhao, X. Li, Z. Yang, D. Zhang, and Z. Liu, "Effect of pore structure on the thermophysical and frictional properties of high-density graphite," *Microporous and Mesoporous Materials*, vol. 330, 2022.
- [24] R. Rajendhiran, V. Deivasigamani, J. Palanisamy, S. Masan, and S. Pitchaiya, "Terminalia catappa and carissa carandas assisted synthesis of TiO₂ nanoparticles - A green synthesis approach," *Materials Today: Proceedings*, vol. 45, pp. 2232–2238, 2021.
- [25] Y. Cao, P. Wang, J. Fan, and H. Yu, "Covalently functionalized graphene by thiourea for enhancing H₂-evolution performance of TiO₂ photocatalyst," *Ceramics International*, vol. 47, no. 1, pp. 654–661, 2021.
- [26] Z. Zhang, Y. M. K. Bader, J. Yang, and L. A. Lucia, "Simultaneously improved chitin gel formation and thermal stability promoted by TiO₂," *Journal of Molecular Liquids*, vol. 328, 2021.
- [27] J. George, C. C. Gopalakrishnan, P. K. Manikuttan, K. Mukesh, and S. Sreenish, "Preparation of multi-purpose TiO₂ pigment with improved properties for coating applications," *Powder Technology*, vol. 377, pp. 269–273, 2021.
- [28] E. M. Hussein, W. M. Desoky, M. F. Hanafy, and O. W. Guirguis, "Effect of TiO₂ nanoparticles on the structural configurations and thermal, mechanical, and optical properties of chitosan/TiO₂ nanoparticle composites," *Journal of Physics and Chemistry of Solids*, vol. 152, 2021.
- [29] G. Li, Y. Sun, Q. Zhang, Z. Gao, W. Sun, and X. Zhou, "Ag quantum dots modified hierarchically porous and defective TiO₂ nanoparticles for improved photocatalytic CO₂ reduction," *Chemical Engineering Journal*, vol. 410, 2021.
- [30] H. Khalid, H. Iqbal, R. Zeeshan et al., "Silk fibroin/collagen 3D scaffolds loaded with TiO₂ nanoparticles for skin tissue regeneration," *Polymer Bulletin*, vol. 78, no. 12, pp. 7199–7218, 2021.
- [31] Y. Sun, G. Li, Y. Gong, Z. Sun, H. Yao, and X. Zhou, "Ag and TiO₂ nanoparticles co-modified defective zeolite TS-1 for improved photocatalytic CO₂ reduction," *Journal of Hazardous Materials*, vol. 403, 2021.
- [32] R. Aswini, S. Murugesan, and K. Kannan, "Bio-engineered TiO₂ nanoparticles using Ledebouria revoluta extract: larvicidal, histopathological, antibacterial and anticancer activity," *International Journal of Environmental Analytical Chemistry*, vol. 101, no. 15, pp. 2926–2936, 2021.
- [33] K. S. Khashan, G. M. Sulaiman, F. A. Abdulameer et al., "Antibacterial activity of TiO₂ nanoparticles prepared by one-step laser ablation in liquid," *Applied Sciences*, vol. 11, no. 10, p. 4623, 2021.
- [34] R. Kaur, A. Kaur, R. Kaur et al., "Cu-BTC metal organic framework (MOF) derived Cu-doped TiO₂ nanoparticles and their use as visible light active photocatalyst for the decomposition of ofloxacin (OFX) antibiotic and antibacterial activity," *Advanced Powder Technology*, vol. 32, no. 5, pp. 1350–1361, 2021.
- [35] O. Ouerghi, M. H. Geesi, E. O. Ibnouf et al., "Sol-gel synthesized rutile TiO₂ nanoparticles loaded with cardamom essential oil: enhanced antibacterial activity," *Journal of Drug Delivery Science and Technology*, vol. 64, 2021.
- [36] J. Singh, S. Juneja, R. K. Soni, and J. Bhattacharya, "Sunlight mediated enhanced photocatalytic activity of TiO₂ nanoparticles functionalized CuO-Cu₂O nanorods for removal of methylene blue and oxytetracycline hydrochloride," *Journal of Colloid and Interface Science*, vol. 590, pp. 60–71, 2021.
- [37] S. Sagadevan, J. A. Lett, G. K. Weldegebrail et al., "Enhanced gas sensing and photocatalytic activity of reduced graphene

- oxide loaded TiO₂ nanoparticles,” *Chemical Physics Letters*, vol. 780, 2021.
- [38] K. N. Pandiyaraj, D. Vasu, R. Ghobeira et al., “Dye wastewater degradation by the synergetic effect of an atmospheric pressure plasma treatment and the photocatalytic activity of plasma-functionalized Cu-TiO₂ nanoparticles,” *Journal of Hazardous Materials*, vol. 405, 2021.
- [39] O. Kose, M. Tomatis, F. Turci et al., “Short preirradiation of TiO₂ nanoparticles increases cytotoxicity on human lung coculture system,” *Chemical Research in Toxicology*, vol. 34, no. 3, pp. 733–742, 2021.
- [40] N. R. Reddy, U. Bharagav, M. M. Kumari et al., “Inclusion of low cost activated carbon for improving hydrogen production performance of TiO₂ nanoparticles under natural solar light irradiation,” *Ceramics International*, vol. 47, no. 7, pp. 10216–10225, 2021.
- [41] A. C. Chu, R. S. Sahu, T. H. Chou, and Y. H. Shih, “Magnetic Fe₃O₄@TiO₂ nanocomposites to degrade bisphenol A, one emerging contaminant, under visible and long wavelength UV light irradiation,” *Journal of Environmental Chemical Engineering*, vol. 9, no. 4, 2021.
- [42] L. Goñi-Ciaurriz, M. Senosiain-Nicolay, and I. Vélaz, “Aging studies on food packaging films containing β-cyclodextrin-grafted TiO₂ nanoparticles,” *International Journal of Molecular Sciences*, vol. 22, no. 5, p. 2257, 2021.
- [43] N. Bono, F. Ponti, C. Punta, and G. Candiani, “Effect of UV irradiation and TiO₂-photocatalysis on airborne bacteria and viruses: an overview,” *Materials*, vol. 14, no. 5, p. 1075, 2021.
- [44] U. Mahanta, M. Khandelwal, and A. S. Deshpande, “TiO₂@SiO₂ nanoparticles for methylene blue removal and photocatalytic degradation under natural sunlight and low-power UV light,” *Applied Surface Science*, vol. 576, 2022.